



# Hydrogeological conceptual model and groundwater recharge of Avella Mts. karst aquifer (southern Italy): A literature review and update

Paola Petrone, Pantaleone De Vita, Palmira Marsiglia, Pasquale Allocca, Silvio Coda\*, Delia Cusano, Daniele Lepore, Vincenzo Allocca\*

Department of Earth Sciences, Environment and Resources, University of Naples Federico II, Monte S. Angelo Campus, 21 Cinthia Street, Building 10, Naples 80126, Italy

## ARTICLE INFO

### Keywords:

Karst aquifer  
Hydrogeological conceptual model  
Groundwater recharge  
Groundwater management

## ABSTRACT

*Study region:* Avella Mts., southern Italy.

*Study focus:* The paper is focused on groundwater of Avella Mts. This aquifer has been experiencing an increasing human pressure due to periods of drought and growth in groundwater extraction. A novel hydrogeological conceptual model was developed, and groundwater recharge was estimated by two approaches. The study was carried out by an in-depth literature review and a GIS-based analysis of geological and piezometric data, ground-based meteorological and remotely sensed data.

*New hydrological insights for the region:* The new hydrogeological conceptual model allowed to reconstruct the aquifer lithology, its deep geometry, and, for the first time, groundwater flow scheme. Five groundwater basins were recognized with distinct outlets and subsurface outflows, suggesting a new aquifer compartmentalization in-series groundwater basins. Some basal springs are fed by autonomous basins with smaller extension, while other springs have dried up completely. The groundwater recharge varies from 7.30 to 6.90 m<sup>3</sup>/s as estimated by Turc formula and MODIS data, respectively; the values are comparable among them, confirming mutually the validity of approaches used. The comparison with previous studies highlights variations and changes for both the hydrogeological conceptual model and water balance, linked to natural and anthropogenic factors. The results obtained represent a way for supporting sustainable management of groundwater, waterwork systems security and groundwater-dependent ecosystems protection of a large sector of Campania region.

## 1. Introduction

Globally 15.2 % of the Earth's land surface is characterized by carbonate rocks and contain abundant groundwater resources (Goldscheider et al., 2020). Approximately about 25 % of the global population depends on karst groundwater (Ford and Williams, 2007). In many countries and regions of the world such as USA (e.g., Texas, Florida), Europe (e.g., Austria, Italy, Dinaric region) and Asia (e.g., China, Lebanon, Syria), karst aquifers massively contribute to the freshwater supply; several large cities, e.g. the city of San

\* Corresponding authors.

E-mail addresses: [silvio.coda@unina.it](mailto:silvio.coda@unina.it) (S. Coda), [vincenzo.allocca@unina.it](mailto:vincenzo.allocca@unina.it) (V. Allocca).

<https://doi.org/10.1016/j.ejrh.2024.101871>

Received 15 February 2024; Received in revised form 20 May 2024; Accepted 13 June 2024

Available online 26 June 2024

2214-5818/© 2024 The Authors. Published by Elsevier B.V. This is an open access article under the CC BY-NC-ND license (<http://creativecommons.org/licenses/by-nc-nd/4.0/>).

Antonio, Miami, Vienna, Rome, Naples, Taiyuan, Beirut, and Damascus entirely depend on karst groundwater (Sun et al., 2020; Chen et al., 2017; Allocca et al., 2014). Karst aquifers hosts important groundwater resources for human consumption, agriculture, industry, cattle farming, energy production, tourism and include cultural heritages, natural landscapes, and ecosystems with great geo- and bio-diversity (Allocca et al., 2018; Goldscheider, 2019).

In Campania region, southern Italy, about 25 % of the land surface is characterized by karst aquifers forming the highest mountain ridges with altitudes up to 1898 m a.s.l.

These aquifers represent the main source for drinking water, agriculture, and industry, and play a vital role for environmental protection and groundwater-dependent ecosystems as Garigliano, Volturno, Sarno and Sele rivers. Historically these aquifers have represented a strategic resource for economic growth and development (Allocca et al., 2014; 2015). In Roman times, some karst springs were captured to feed by Augustan aqueduct (33 – 12 BC) cities such as *Neapolis*, *Puteoli*, *Pompeii*, *Cumae* and *Beneventum* (Cusano et al., 2023). In the post-Second World War period, karst groundwater has certainly favored the economic growth,

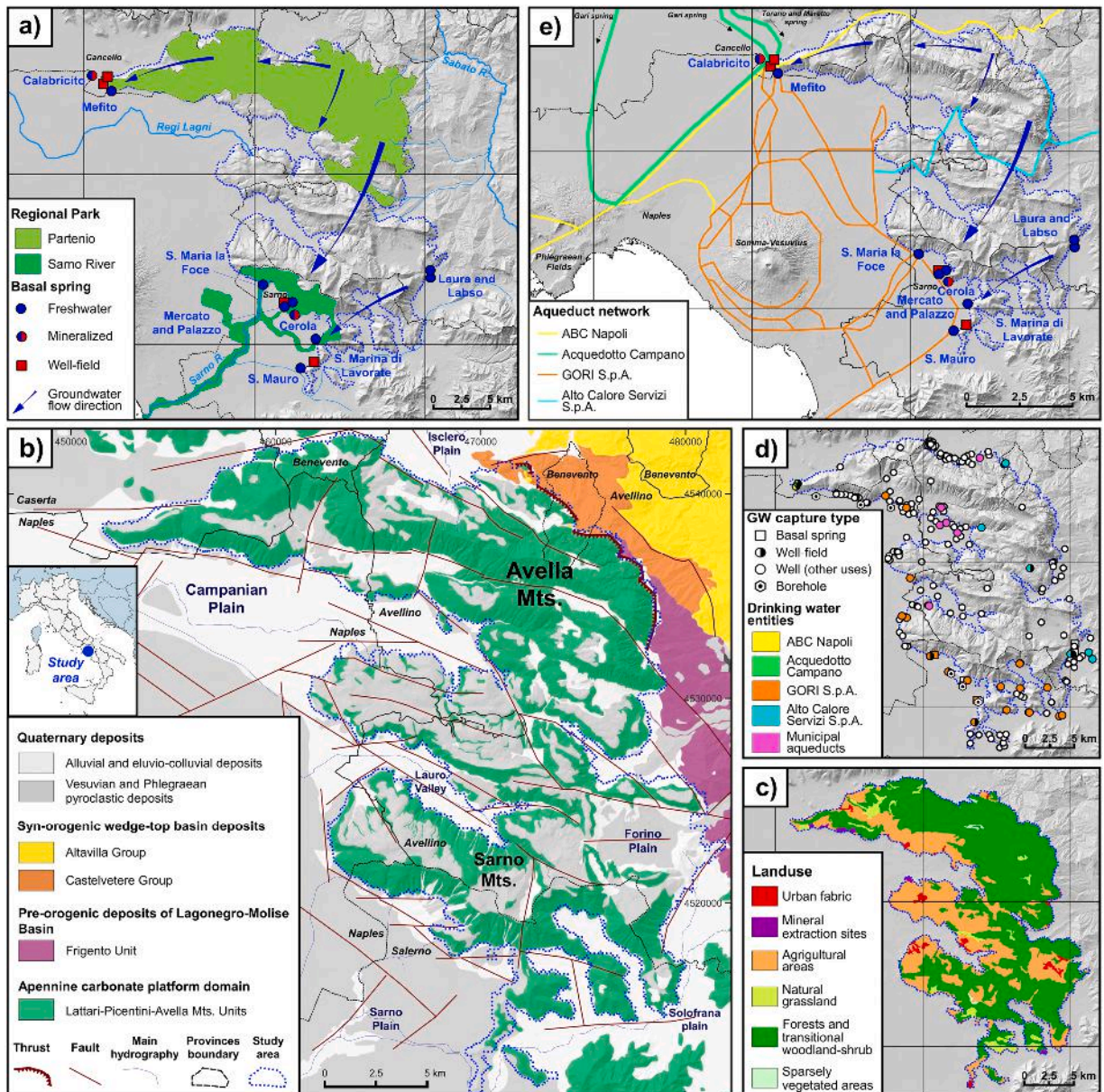


**Fig. 1.** Location of the study area. a) Avella Mts., Partenio and Sarno River Regional Parks, and groundwater-dependent ecosystems (<https://www.sciencedirect.com/topics/earth-and-planetary-sciences/groundwater-dependent-ecosystem>) of Sarno, Sabato and Regi Lagni rivers; b) Geological map (from Vitale and Ciarcia, 2018, modified); c) Corine Land Cover (2018) simplified; d) Well-fields, wells, boreholes, and basal springs used for drinking water supply by public bodies, companies and private users; e) Tapped basal springs and aqueduct systems.

industrialization, infrastructure development and improvement of living conditions of the Campanian population. This was possible thanks to mean annual specific groundwater recharge (up to  $0040 \text{ m}^3/\text{s}/\text{km}^2$ ) among the highest in Italy, being linked to high permeability of karst rocks, high rates of precipitation, endorheic areas, and permeable pyroclastic soils covered by dense deciduous forest that favour groundwater recharge (Allocca et al., 2014; 2015; Fusco et al., 2017; De Vita et al., 2018; Cusano et al., 2024). Huge basal springs have a high average annual flow rate (up to about  $6 \text{ m}^3/\text{s}$ ) and excellent hydrochemical quality, feeding rivers, lakes, wetlands, and coastal areas. However, these karst aquifers are particularly vulnerable to pollution and human impacts (Tufano et al., 2020; Cusano et al., 2023) and, in some cases, it is difficult to implement effective protection strategies that involve strong restrictions on both land use and anthropogenic activities (Allocca et al., 2018; Cusano et al., 2023). The strongly space-time climatic variability of Campania region related to the North Atlantic Oscillation (De Vita et al., 2012) determine a significant inter-annual variation of groundwater recharge and spring discharges, and consequently a reduction in groundwater availability for regional and local water network systems.

For these reasons, the risk to unbalance between groundwater supply and demand is high, as already experienced in water-emergencies occurred in 2000, 2011, 2017 and 2020 in the Naples metropolitan area, where highest drinking-water demand occurs. In this densely populated area (total inhabitants about 3.2 million) of Campania region, during the last decades, the human pressure and aquifer exploitation rate are strongly increasing as resulting from inter-annual meteorological drought periods. Thus, in addition to the large basal springs captured for drinking water use, numerous private wells (in some cases even unauthorized) and well-fields were drilled for drinking, agriculture, industry, and other water supplies (Allocca et al., 2007).

Moreover, the water withdrawals from these wells occur through an uncoordinated management among the regional and provincial public bodies, in charge to give permissions to groundwater exploitation, and above all not based on an updated conceptual hydrogeological model and water balance.

In a such complex hydrogeological scenario, the need of a revisited hydrogeological conceptual model and updated water balance is an urgent issue to be addressed to prevent overexploitation of aquifers (Lancia et al., 2020; Ben Saad et al., 2023), in agreement with water policies of the UN 2030 Agenda for Sustainable Development and Water Framework Directive 2000/60/EC.

The Avella Mts. karst aquifer was selected among the others of the Campania region because supplying numerous urban centers of Naples, Caserta, Avellino, Salerno and Benevento provinces and the human pressure and aquifer exploitation rate are strongly increased in the last decades. Based on an in-depth literature review, the aim of this study was to reconstruct a novel hydrogeological conceptual model of Avella Mts. by new geological and hydrogeological data and estimate groundwater recharge by a water balance based on both ground-based meteorological observations and remotely sensed data.

The remaining of the paper is organized as follows: Section 2 describes the geological and hydrogeological characteristics of the study area, as well as spring tapping works, waterworks, and groundwater use; Section 3 provides a literature review regarding previous hydrogeological schemes and water balances; Section 4 shows the data and methodological approaches used; Sections 5 and 6 comment the obtained results and provide their discussion, while Section 7 reports the concluding remarks.

## 2. Study area description

### 2.1. Geological and hydrogeological setting

The Avella Mts. extending approximately  $370 \text{ km}^2$  are located within Partenio and Sarno River Regional Parks and shared by all five provinces of the Campania region (Fig. 1a and b).

This large carbonate ridge hosts a karst aquifer system with a mean annual specific groundwater recharge (up to  $0.037 \text{ m}^3/\text{s}/\text{km}^2$ ) among the highest in the southern Apennine and sustaining a series of ecosystem services. A large Site of Community Importance (<https://www.mase.gov.it/pagina/rete-natura-2000>) and numerous environments and ecosystems, e.g., forests, grasslands, springs, rivers, poljes and other karst landforms contribute to its variegated and wide geo- and biodiversity. Surface and groundwater resources play a primary role in the regulation of the hydro-ecological regime of Sarno, Regi Lagni and Sabato rivers (Fig. 1a).

From a hydrogeological point of view, the Avella Mts. are a well-defined karst aquifer (Celico, 1983), delimited to the west by the Campanian plain, to the north and south by the alluvial plains of Isclero and Solofrana rivers, respectively (Fig. 1b). The massif is constituted mainly by a fractured and karstified Mesozoic-Cenozoic carbonate series of the Apennine platform domain belonging to the "Monti Picentini and Lattari" and "Monti di Avella" tectonic units (ISPRA, 2017), characterized from bottom to top by Norian-Hettangian dolomites, Jurassic-Lower Cretaceous dolomitic limestones, and Cretaceous limestones, faulted and fractured by a complex network of discontinuity NW-SE and SW-NE oriented (Vitale and Garcia, 2018). The carbonate hydrostructure is hydraulically confined by low permeability terrigenous units belonging to synorogenic wedge-top basin deposits laterally juxtaposed by thrust, and alluvial deposits and Vesuvian and Phlegraean ash-fall and ash-flow pyroclastic deposits in tectonic contact by normal faults (Fig. 1b).

In such a hydrogeological framework, Avella Mts. are characterized by a basal groundwater flow orientated towards three main spring groups (Fig. 1a): i) Cannello spring group located in the north-western sector, originally was characterized by Calabricito and Mefito springs (30 and 28 m a.s.l.); ii) Sarno spring group located in the southern sector, originally represented by S. Maria La Foce (32 m a.s.l.), Mercato, Palazzo (26 and 24 m a.s.l.), Cerola (28 m a.s.l.), S. Marina di Lavorate (28 m a.s.l.) and S. Mauro springs (27 m a.s.l.); iii) Laura and Labso springs (185 and 199 m a.s.l.) located in the south-eastern sector.

Systematic flow measurements carried out in the 1960s and 1970s by National Hydrological Service - Department of Naples (Celico, 1983; Allocca et al., 2007) allowed to estimate the following average spring discharges:  $1.20 \text{ m}^3/\text{s}$  for the Calabricito and Mefito springs;  $2.60 \text{ m}^3/\text{s}$  for the S. Maria La Foce spring;  $3.00 \text{ m}^3/\text{s}$  for the Mercato and Palazzo springs;  $0.60 \text{ m}^3/\text{s}$  for the Cerola spring;  $1.80 \text{ m}^3/\text{s}$  for the Santa Maria di Lavorate spring;  $0.40 \text{ m}^3/\text{s}$  for the San Mauro spring;  $0.25 \text{ m}^3/\text{s}$  for the Laura and Labso springs.

These basal springs are characterized by freshwater (electrical conductivity between 670 and 1020  $\mu\text{S}/\text{cm}$ ) with an excellent hydrochemical quality and a typically bicarbonate-calcium composition that reflects the aquifer lithology (Celico et al., 1980). High content of endogenous  $\text{CO}_2$  (up to 330 ppm) that characterizes the Calabricito and Cerola highly mineralized springs (electrical

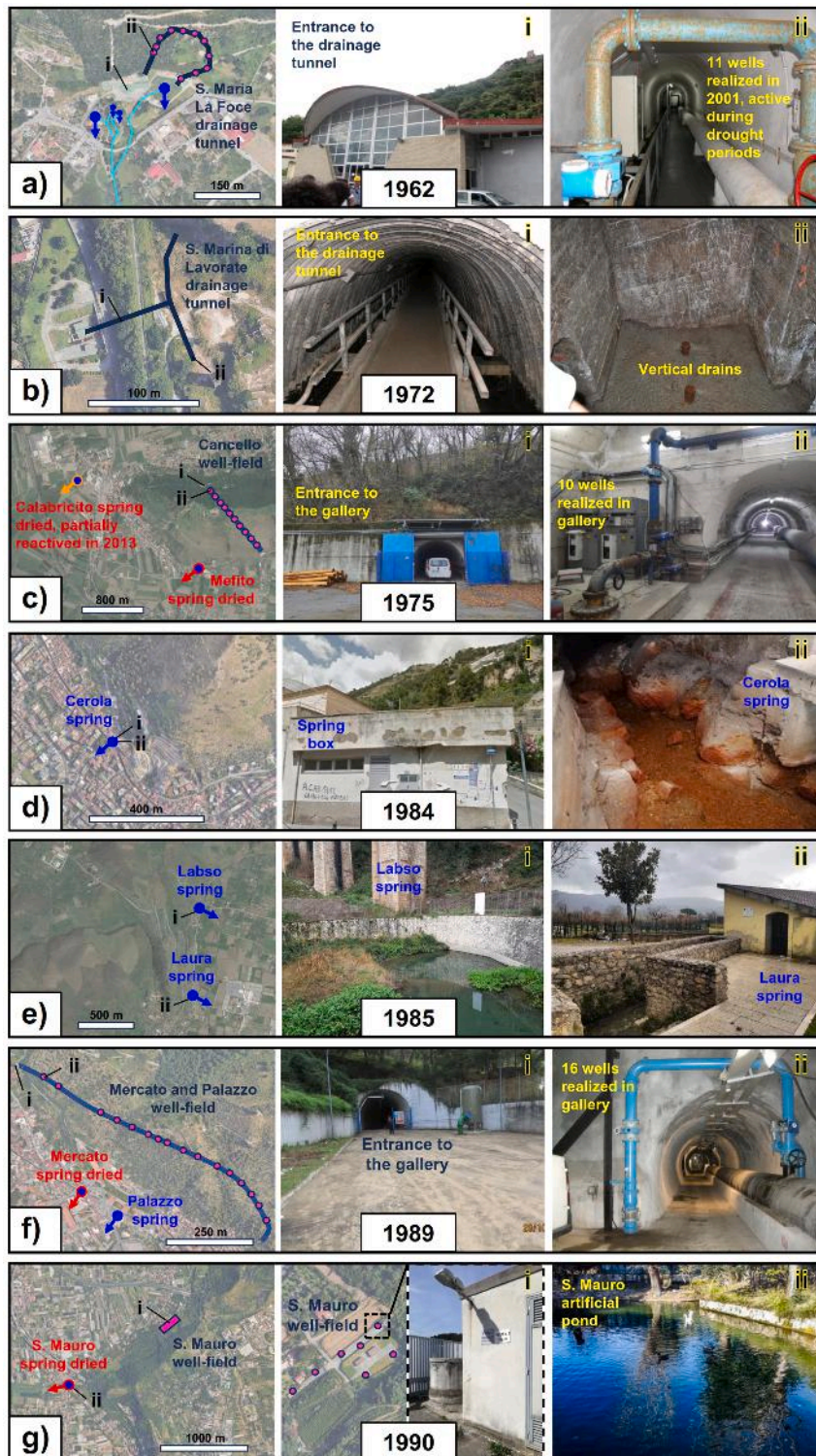


Fig. 2. Location sketch, date of construction, and characteristics of basal spring tapping works. a) S. Maria La Foce spring; b) S. Marina di Lavarate spring; c) Mefito and Calabricito springs; d) Cerola spring; e) Laura e Labso springs; f) Mercato and Palazzo springs; g) S. Mauro spring.

conductivity up to 2130  $\mu\text{S}/\text{cm}$  (Fig. 1a) are linked to gas rise through deep normal faults which interacts locally with deep and shallow groundwater of the karst aquifer (Celico et al., 1980).

Given the proximity to the volcanic centers of Somma-Vesuvius and Phlegraean Fields, the karst aquifer is singularly covered (Fig. 1b and e) by alkali-potassic ash-fall pyroclastic deposits with thickness up to about 8 m along slopes, where the slope angle is greater (up to  $40^\circ$ ), and about 50 m, in summit flat and endorheic areas (Fusco et al., 2017). Along the steep slopes, dense deciduous forests and transitional woodlands constitute the predominant types of land use and vegetation cover, while in the endorheic karst areas and in the piedmont sectors, agricultural areas (chestnuts and hazelnuts), natural grassland and subordinately urban areas are prevalent (Fig. 1c).

The climate is Mediterranean-mild type (CSb) (Beck et al., 2018), whereas mean annual rainfall and air temperature are equal to 1700 mm/y and  $13,4^\circ\text{C}$ , respectively (Allocca et al., 2014; Ruggieri et al., 2021).

## 2.2. Groundwater development growth

Since the 1960s groundwater of Avella Mts. (Fig. 1d) has played a strategic role in socioeconomic growth and development of the Campania region. In the post-Second World War period, water demand of the Naples metropolitan area has significantly increased, due to industrialization, urbanization, and population growth. Given the excellent hydrochemical quality of the groundwater, some basal springs originally used by local farmers for irrigation were tapped and exploited for drinking water supply (Fig. 2). Thus, in the framework the Special Project 29 the Cassa per il Mezzogiorno Italian Government Agency were financed and constructed the Campanian aqueduct (Acquedotto Campano; Fig. 1e) and the so-called Sarno aqueduct (GORI SpA; Fig. 1e) for the water supply of Naples metropolitan district, including the peri-vesuvian area.

In 1962 and 1972 two drainage tunnels were constructed (Fig. 2a and b) each with a total length of about 0.30 km, to tap water of S. Maria La Foce and S. Marina di Lavorate springs (Civita et al., 1969a; 1969b). Both tunnels were excavated with sub horizontal inclination, about 28 and 26 m a.s.l., respectively, i.e., a few meters below the natural altitude of basal springs (32 and 28 m a.s.l.). In the summer of 2001, after a meteorological drought period the drainage tunnel of S. Maria La Foce spring dried up totally; thus, eleven wells were drilled inside the tunnel (Fig. 2a) to compensate the flow rate during periods of drought such as those occurred again in 2011, 2017, and 2020.

In the meantime, three well-fields were drilled upstream of Mefito, Calabricito, Mercato, Palazzo and S. Mauro springs in 1975, 1989 and 1990, respectively (Fig. 2c, f and g). The activation of these well-fields led to the drying up of Mefito, Calabricito, Mercato and S. Mauro springs. Instead, the Cerola, Laura and Labso springs were tapped in the first half of the 1980s for agricultural use by gravity intake systems (Fig. 2d and e).

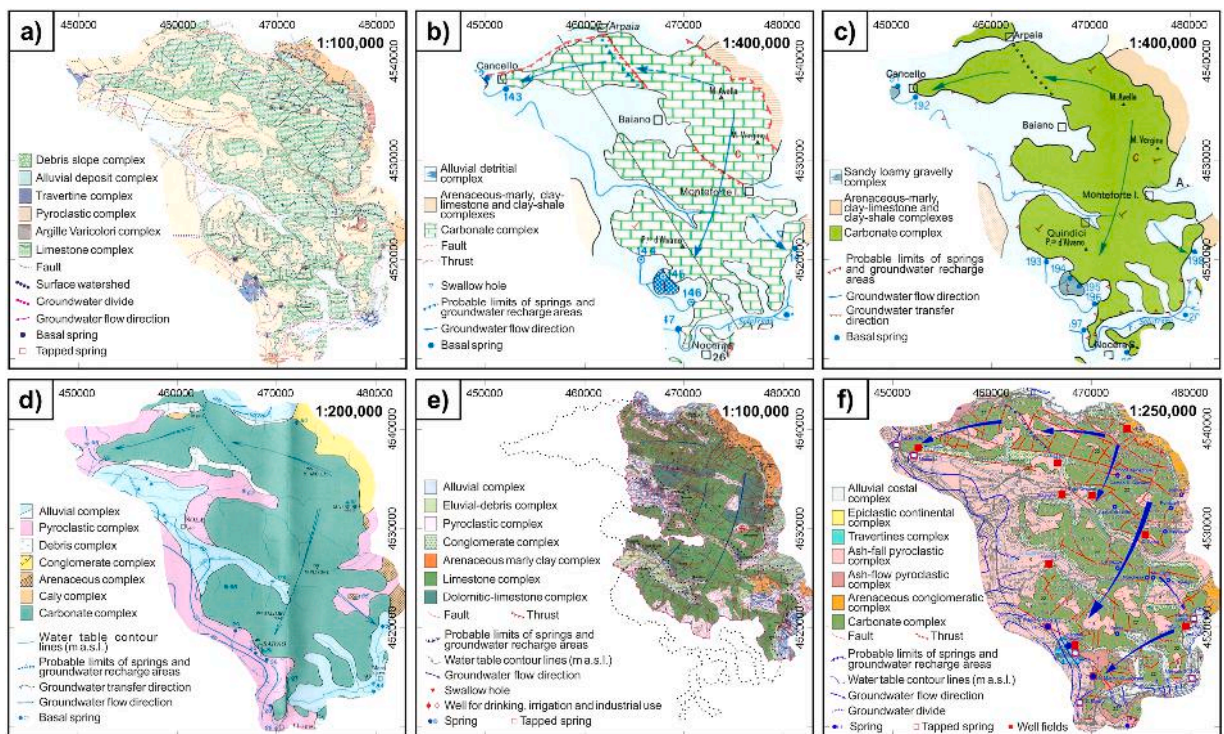


Fig. 3. Previous hydrogeological schemes of Avella Mts.: a) from Civita et al. (1973) modified; b) from Celico (1978) modified; c) from Celico (1983) modified; d) from Budetta et al. (1994) modified; e) from Allocca et al. (2008) modified; f) from De Vita et al. (2018) modified.

**Table 1**

Summary table of previous water balances of Avella Mts. P, mean annual precipitation; T, mean annual air temperature; AET, mean annual actual evapotranspiration; GR, mean annual groundwater recharge; GRC, Groundwater Recharge Coefficient; SGR, mean annual Specific Groundwater Recharge (mean annual groundwater recharge for unit area); \* No. of stations used to reconstruct distributed models of P and T at the regional scale; (C) Coutagne; (T) Turc; (TM) Thornthwaite-Mather; (M) MODIS; (\*\*) average value.

References	Water balance	Area (km <sup>2</sup> )	Scale of analysis	Period	No. of stations		P (mm)	T (°C)	AET (mm)	GR (mm)	GRC	GR (m <sup>3</sup> /s)	SGR (m <sup>3</sup> /s/km <sup>2</sup> )
					p	T							
<a href="#">Civita et al. (1970)</a>	1	361	1:200,000	1968÷1969	11	7	1842	14.3	740	1161	1	13.30	0.037
<a href="#">Celico and de Riso (1978)</a>	2	360	1:300,000	1921÷1955	15	7	1339÷1477 (1408 <sup>**</sup> )	13.5	590÷638 (614 <sup>**</sup> )	790	1	8.50÷9.20 (8.85 <sup>**</sup> )	0.024÷0.026 (0.025 <sup>**</sup> )
<a href="#">Allocca et al. (2014)</a>	3	334	1:250,000	1921÷2012	387*	228*	1437	12.7	454 660 (C) 692 (T)	602 636 (C) 564 (T)	1÷0.57	6.38 6.74 (C) 5.97 (T)	0.019 0.020 (C) 0.018 (T)
<a href="#">Ruggieri et al. (2021)</a>	4	334	1:250,000	2000÷2014	266*	150*	1476	13.6	747 (TM) 711 (M) (703 <sup>**</sup> )	515 (TM) 522 (M) (559 <sup>**</sup> )	1÷0.57	5.46 (TM) 5.53 (M) (5.93 <sup>**</sup> )	0.016 (TM) 0.017 (M) (0.018 <sup>**</sup> )

Starting from the 1990s and 2000s further wells and well-fields were drilled by public agencies and joint-stock companies for drinking water supply (Fig. 1d). Today, the entire volume of groundwater exploited for drinking water supply, totaling about  $198 \times 10^6$  m<sup>3</sup>/y, is distributed by four main regional and provincial waterworks (Fig. 1e; GORI SpA, Acquedotto Campano, ABC Napoli, Alto Calore Servizi SpA) and some municipal aqueducts (Fig. 1d) to feed a large area of the Campania region with a population of approximately four million inhabitants.

Contextually, starting from the 1990s and 2000s numerous private wells have drilled in the piedmont karst areas for agriculture, industry, domestic and other private uses (Fig. 1d) of whose withdrawal rates are not known. All these wells have resulted in a strong increase of groundwater exploitation whose critical effects were enhanced by drought periods and an uncontrolled and uncoordinated groundwater management.

### 3. Literature research and review

#### 3.1. Previous hydrogeological maps

Starting from the 1970s some conceptual hydrogeological model and groundwater circulation schemes of Avella Mts. were published with different hydrogeological information.

The first scheme at the 1:100,000 scale (Fig. 3a) is shown on the hydrogeological map of north-western Campania region (Civita et al., 1973), in which three hydrogeological complexes were identified, i.e., limestone, pyroclastic and debris slope complexes. Based on a geomorphological criterion, the hydrogeological scheme shows a local correspondence between watershed and hydrogeological boundaries. In addition to the hydrogeological limits of groundwater basins of Cancellito and Sarno springs, the occurrence of other small groundwater basins was hypothesized, in the north-eastern sector where historically the basal springs have never recognized.

Subsequently, in the framework of the hydrogeological map of the central-southern carbonate Apennine (Celico, 1978) a new scheme is proposed at the 1:400,000 scale (Fig. 3b) based on a hydrogeological and hydrostructural criterion coupled with magnitude of spring discharges (Celico, 1983). Although characterized by lesser geological information (a unique carbonate complex is mapped), two main large groundwater basins were identified and no correspondence among hydrographic and hydrogeological boundaries is proposed. The basal groundwater flow is split into two main directions (Fig. 3b); the first N-W oriented, towards the Cancellito spring group, and the second southward directed, towards the Sarno spring group, and subordinately Laura and Labso springs. Conversely, the thrust occurring along north-eastern edge of massif was interpreted as a no-flow boundary as well as inverse faults within the carbonate ridge were considered as probable limit of groundwater basins feeding springs.

In the two subsequent schemes (Fig. 3c and d) implemented at the 1:400,000 (Celico, 1983) and the 1:200,000 scale (Budetta et al., 1994), respectively, the previous hydrogeological scheme (Celico, 1978) is confirmed, and some information about outflow from carbonate to alluvial-pyroclastic complex are indicated. Moreover, based on hydrochemical and isotopic spring data (Celico et al., 1980) a possible outflow from the Solofrana plain to the carbonate complex has been also hypothesized.

A partial scheme at the 1:100,000 scale (Fig. 3e) is proposed within of the hydrogeological map of Avellino province (Allocca et al., 2008). In addition to hydrogeological complexes and groundwater flow scheme, the high-altitude springs and main drinking, agricultural, and industrial wells are also reported.

Recently, a scheme at the 1:300,000 scale (Fig. 3f) was realized in the framework of the hydrogeological map of continental southern Italy (Allocca et al., 2007; De Vita et al., 2018), which provided an update of the basal and perched spring discharges, as well as location of main drinking well-fields.

In all hydrogeological schemes there is missing data about the morphology of the piezometric surface of basal water table, as well as information on hydraulic gradients, extension of groundwater basins feeding basal springs, based on piezometric data and groundwater flow path. This represents a lack of information affecting generally the karst aquifers of southern Italy, whose impervious mountain morphology prevents the drilling of very deep water wells.

#### 3.2. Previous water balances

In the last 60 years, starting from the preparatory surveys aimed at the design of tapping works of basal springs (Nicotera and Civita, 1969a; 1969b; Civita et al., 1970; Civita et al., 1973), the groundwater recharge (GR) of Avella Mts. was estimated by different dataset and methodologies, as well as different periods and scale of analysis (Table 1). The previous estimates of GR were carried out by an empirical method based on the multiplication of actual precipitation, namely precipitation minus actual evapotranspiration, by a Groundwater Recharge Coefficient (GRC), whose complement represent the runoff coefficient.

Civita et al. (1970) estimates the GR for 1968÷1969 hydrologic year. Using ground-based hydrological data of 11 precipitation gauges and 7 air temperature stations, and by application of Thiessen method and Turc's (1954) formula, the GR was evaluated in 13.30 m<sup>3</sup>/s by the estimate of effective precipitation and GRC equal to 1, thus considering the runoff as null (Table 1).

Celico and de Riso (1978) estimated the mean annual GR for the period 1921÷1955 by rainfall and air temperature data of 15 meteorological stations and applying Thiessen and isohyetal methods, and Turc's formula. The mean annual GR was estimated varying between 8.50 and 9.20 m<sup>3</sup>/s, depending on the spatialization technique used and considering negligible the runoff (i.e., GRC equal to 1).

Allocca et al. (2014) estimate the mean annual GR for the period 1926÷2012 using for first time a GIS-based procedure and a methodological approach that considers the role of the aquifer lithology, cover soil type, land use, and endorheic areas. By a large dataset of meteorological stations and regional distributed models of precipitation and air temperature, the GR was estimated equal to

6.38 m<sup>3</sup>/s, by the calculation of actual evapotranspiration by Turc’s empirical formula and considering a GRC equal to 1 and 0.57 for endorheic and open slope areas, respectively (Table 1).

Ruggieri et al. (2021) estimate the mean annual GR for the period 2000÷2014 by ground-based hydrological and satellite data. By a GIS-based procedure and regional regression models of precipitation and air temperature, the GR was estimated equal to 6.74, 5.97, 5.46, and 5.53 m<sup>3</sup>/s by means of the empirical formulas of Coutagne (1954), Turc (1954), Thornthwaite, Mather, (1955) and MODIS data, respectively, and considering a GRC equal to 1 and 0.57 for endorheic and open slope areas as described in Allocca et al. (2014).

Based on these estimates, the mean annual Specific Groundwater Recharge (SGR) of Avella Mts. varies from 0.016 to 0.037 m<sup>3</sup>/s/km<sup>2</sup> (Table 1).

All other hydrological data and relative scale of analysis, different methods and results of water balances have been summarized in Table 1.

#### 4. Data and methodology

In the Fig. 4 is shown a flowchart containing the sources, input data, processing, and outputs to develop the novel conceptual hydrogeological model and the twofold water balance.

All data and each step of performed procedures are described in the following paragraphs.

##### 4.1. Geological and hydrogeological data

By a GIS-based procedure, a novel hydrogeological conceptual model of Avella Mts. was implemented using new and open-sources geological data of the CARG project (Sheets No. 431, 432, 448, 449, 466, 467, 485; ISPRA, 2017), literature data, field measurements, as well as unpublished stratigraphic, spring and piezometric data contained in institutional archives and national databases.

All sources and data collected (Table 2) was stored in a hydrogeological geospatial database.

Using a WGS84-UTM33N projected coordinate system during the processing phase (Fig. 4), all geological data were digitized in a CAD environment, assigning an ID code to each geological formation. In accordance with the method described in De Vita et al. (2018), the geological formations were divided based on sedimentation domain, lithology, structural and hydrogeological characteristics, age, and merged into hydrostratigraphic units (Maxey, 1964; Seaber, 1988). These hydrostratigraphic units, also referred to as hydrogeological complexes (Celico, 1986), are defined as a series of lithotypes or formations with a proved spatial and structural unity, an analogous type of relative permeability and a permeability grade ranging in a restricted interval. Thus, to each hydrogeological complex a type and grade of porosity and relative permeability, range of hydraulic conductivity (Freeze and Cherry, 1979; Civita, 2005) and hydrogeological role were assigned.

For the first time, an unreleased groundwater flow scheme was implemented by a piezometric contour map of the basal water table. This represents a novelty for the Avella Mts. and, in general, for southern Italy, if considering the lack of piezometric data in the inner part of mountainous karst aquifers. In total, hydraulic heads data of eight basal springs and two hundred and twelve wells and boreholes (Fig. 1d) were acquired during a new census and piezometric investigations carried out in the period 2019÷2020, measuring: i) geographic coordinates and elevation of springs and wells (m a.s.l.) by a portable differential GPS (K9 Series RTK, KOLIDA Instrument, China), and ii) depth of piezometric levels (m b.g.l.) in public and private wells using a water level indicator (BFK-

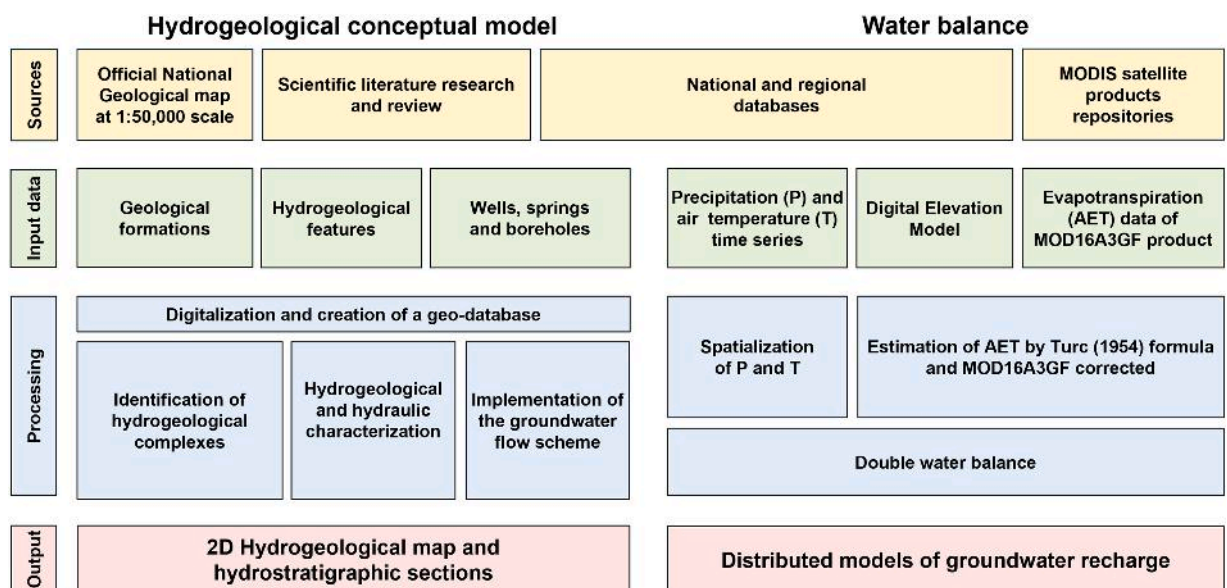


Fig. 4. Flow chart showing the workflow developed for the definition of the hydrogeological conceptual model and water balance of Avella Mts.



**Table 2**

Hydrogeological domains, characteristics, and hydraulic properties of hydrogeological complexes of Avella Mts. (P) Porosity; (F) Fracturing; (K) Karst; (F<sub>W</sub>) Freshwater; (M<sub>W</sub>) Mineralized water.

Hydrogeological domain	Hydrostratigraphic unit/ Hydrogeological complex			Degree and type of relative permeability	Hydraulic conductivity (m/s)	Hydrogeological role	GW type	Area (% of total)
	ID	Litology	Age					
Quaternary deposits	1	Eluvial-colluvial	Holocene-Present	Medium (P)	$10^{-9} \div 10^{-5}$	Aquitard	F <sub>W</sub>	2.7
	2	Lacustrine and marshy	Early Pleistocene-Present	Medium (P)	$10^{-9} \div 10^{-4}$	Aquifer/aquitard	F <sub>W</sub>	1.3
	3	Pyroclastic-alluvial	Late Pliocene-Present	Medium (P)	$10^{-6} \div 10^{-3}$	Aquifer	F <sub>W</sub>	4.6
	4	Detrital	Late Pleistocene-Present	Medium (P)	$10^{-6} \div 10^{-3}$	Aquifer	F <sub>W</sub>	9.0
	5	Travertine	Holocene	Medium (P)	$10^{-6} \div 10^{-3}$	Aquifer	F <sub>W</sub> , locally M <sub>W</sub>	< 0.1
	6	Pyroclastic deposits	Late Pleistocene-Holocene	Medium (P)	$10^{-9} \div 10^{-3}$	Aquifer/aquitard	F <sub>W</sub>	27.6
	7	Tuff	Late Pleistocene-Holocene	Low (P and F)	$10^{-9} \div 10^{-4}$	Aquitard	F <sub>W</sub>	0.1
Turbiditic pre- and syn-orogenic deposits	8	Sandstone	Late Miocene-Late Pliocene	Low (P and F)	$10^{-9} \div 10^{-6}$	Aquiclude	\	0.9
	9	Argille Varicolori	Oligocene-Early Miocene	Low (P and F)	$10^{-10} \div 10^{-7}$	Aquiclude	\	
Mesozoic-Cenozoic carbonate platform succession	10	Limestone	Middle Jurassic-Early Miocene	Very high (F and K)	$10^{-3} \div 1$	Aquifer	F <sub>W</sub> , locally M <sub>W</sub>	19.5
	11	Orbitolina limestone and marl	Early Cretaceous	Low (F)	$10^{-9} \div 10^{-6}$	Aquitard		< 0.1
	12	Limestone-dolomite	Late Triassic-Late Cretaceous	Very high (F and K)	$10^{-3} \div 1$	Aquifer	F <sub>W</sub> , locally M <sub>W</sub>	33.3
Lagonegro-Molise Basin Units	13	Dolomite	Late Triassic-Early Jurassic	Medium (P and F)	$10^{-6} \div 10^{-3}$	Aquifer	F <sub>W</sub> , locally M <sub>W</sub>	0.3
	14	Marly limestone	Eocene-Early Miocene	Low (P and F)	$10^{-9} \div 10^{-6}$	Aquiclude	\	0.3
	15	Siliceous-marly	Middle Triassic-Early Cretaceous	Low (P and F)	$10^{-10} \div 10^{-7}$	Aquiclude	\	

100 model, PASI, Italy). The field measurements were integrated with available data from online national database (<http://portalesgi.isprambiente.it/>), institutional archives and literature data. All piezometric data (Fig. 1b and d) were interpolated and spatialized through the Triangulated Irregular Network method, using SURFER software.

Moreover, an in-depth census of the high-altitude springs and a mapping of surface karst landforms was carried out, by an analysis of digital regional technical cartography at the scale 1:5000, supported by field survey and uploading the literature data and inventory of karst caves of Campania region (<http://www.fscampania.it/catasto-2/catasto/>).

All geological and hydrogeological data were merged into a novel hydrogeologic conceptual model (Fig. 5), represented by a hydrogeological map at the scale 1:50,000 and two hydrostratigraphic sections reconstructed based on literature data and new boreholes.

#### 4.2. Updated water balance

The mean annual GR was estimated by an updated water balance for the 2000–2019 period, starting from the following equation:

$$P = AET + R + GR \pm \Delta W_r \quad (1)$$

where P (mm/y) is mean annual precipitation, AET (mm/y) is the mean annual actual evapotranspiration, R (mm/y) is the mean annual runoff, GR (mm/y) is the mean annual GR, and  $\pm \Delta W_r$  (m<sup>3</sup>) is the inter-annual variation of groundwater reserves, the latter considered negligible in the long-term timescale.

Time series of precipitation and air temperature of 23 rain gauges and 11 air temperature stations (Fig. 6) were acquired from regional hydro-meteorological monitoring network of the Civil Protection of Campania Region. All sources and input data collected

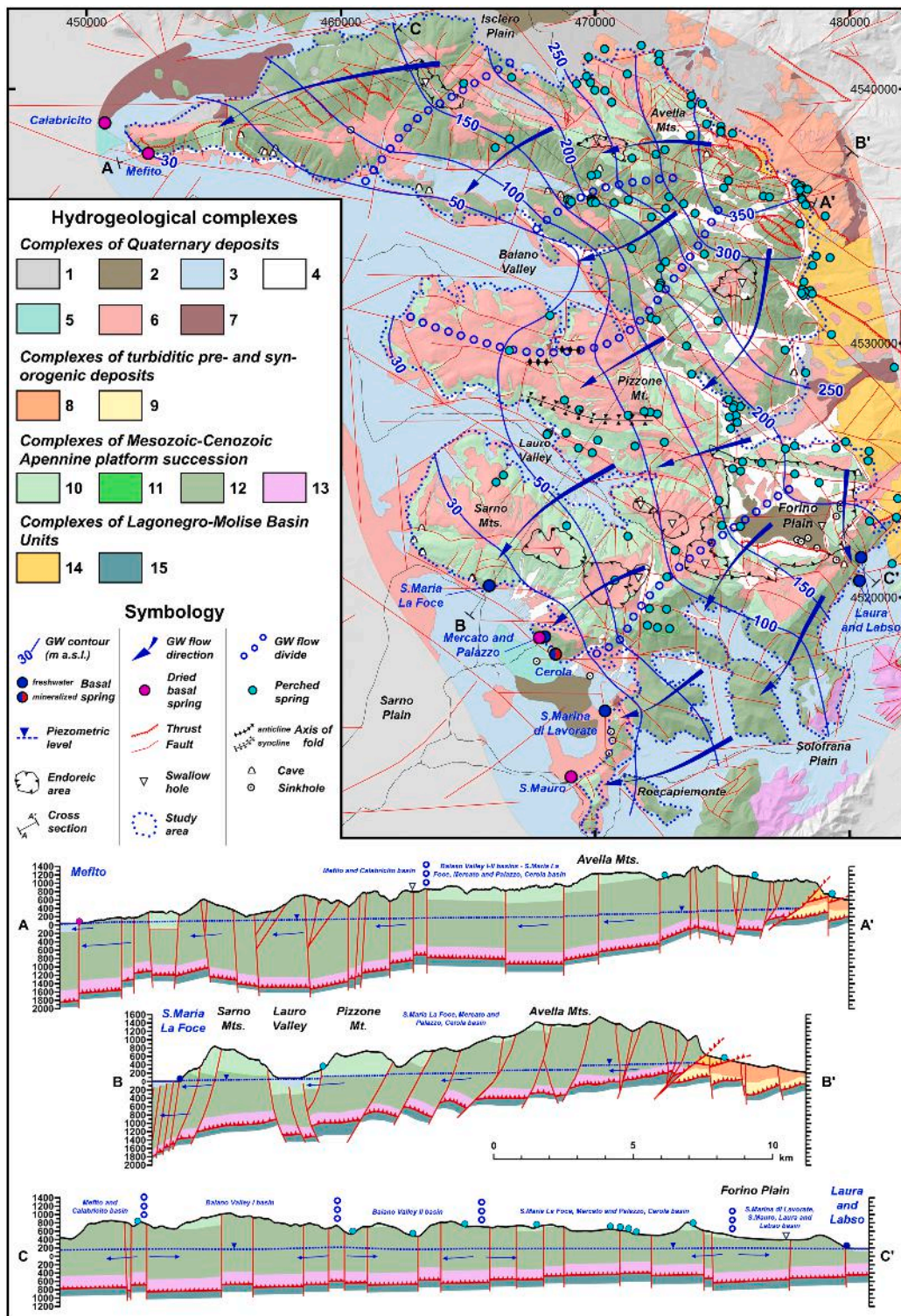


Fig. 5. Novel hydrogeological conceptual model of Avella Mts. In the Table 2 the description of hydrogeological complexes is reported.

(Table 2) were stored in a hydrogeological database.

Two linear models for rainfall-altitude and air temperature-altitude relationship were reconstructed (Fig. 6) by a linear regression methodology, and applied on a DEM with a resolution of 10 m. Subsequently, the distributed models of mean annual precipitation and mean annual air temperature were upscaled at a resolution of about 500 m, likewise the actual evapotranspiration and groundwater

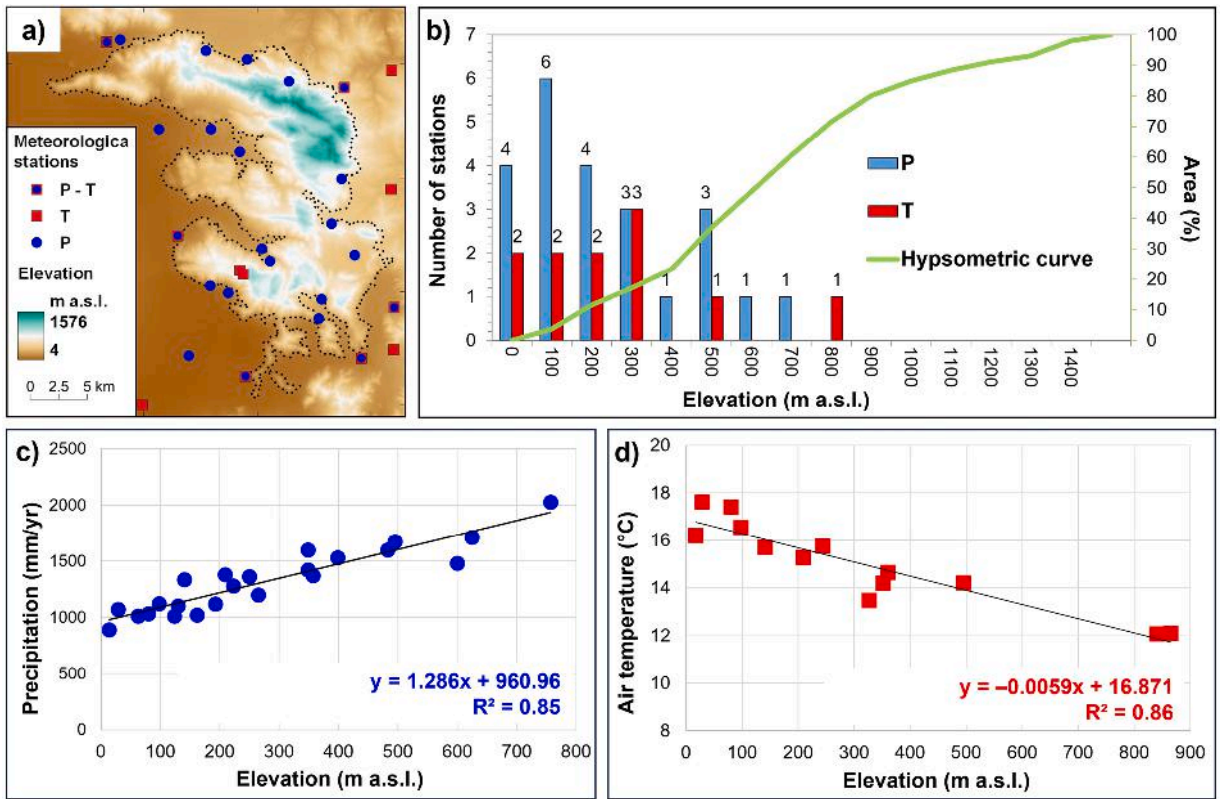


Fig. 6. a) Planimetric distribution of the meteorological stations network; b) Hypsometric curve and distribution of gauges with altitude; c) Linear regression model of mean annual precipitation (2000–2019 period); d) Linear regression model of mean annual air temperature (2000–2019 period).

recharge.

In order to make a comparison between previous and new results, the AET has been estimated empirically by Turc’s (1954) formula:

$$AET = \frac{P}{\sqrt{0.9 + \left(\frac{P}{300 + 25T + 0.05T^3}\right)^2}} \tag{2}$$

where P (mm/y) and T (°C) are the mean annual precipitation and mean annual air temperature, respectively. A value of AET equal to 0 was assigned to non-vegetated areas, identified by the Corine Land Cover (2018) dataset at the 1:250,000 scale of the Copernicus Land Monitoring Service (<https://land.copernicus.eu/en>) and verified through satellite images from Google Earth.

Moreover, the AET was evaluated by the Terra Moderate Resolution Imaging Spectroradiometer (MODIS) dataset which includes meteorological variables, land cover and soil type (Mu et al., 2011). The product employed was MOD16A3GF v061 (Running et al., 2021) available at native resolution of 500 m, which provides data generated by an algorithm based on the Penman-Monteith equation (Monteith, 1965). The yearly AET maps were downloaded, converted to tiff format, and reprojected to WGS84-UTM33N system, using a R package named MOD1Stp (Busetto and Ranghetti, 2016). Each raster underwent processing in according to the user’s guideline of the MOD16A3GF product (Running et al., 2021), assigning a value equal to 0 for non-vegetated areas or with low-quality acquisition, and converting the unit of measure from kg/m<sup>2</sup>/y to mm/y. The mean annual AET raster was computed as arithmetic average of yearly AETs.

Lastly, starting from the general water balance Eq. (1), the mean annual GR has been estimated empirically by following formula:

$$GR = (P - AET) \times GRC \tag{3}$$

where GRC (dimensionless) is groundwater recharge coefficient, equal to 0.57 to open slopes with a slope angle greater than 5° (Allocca et al., 2014), while equal to 1 and 0 to endorheic and urban impervious areas, respectively. The outputs were two distributed models of mean annual GR calculated by both AET estimations (Fig. 4). Coupled use of terrestrial and satellite data was found to be an attractive approach, reducing uncertainties, and having a mutual control in the estimate of groundwater recharge.

## 5. Results

### 5.1. Hydrogeological conceptual model

In Table 2 and Fig. 5 the summary of the novel hydrogeological conceptual model is presented.

At the 1:50,000 scale, it was possible to recognize 15 hydrogeological complexes belonging to four hydrogeological domains, 13 of which are outcropping and two buried (see section A-A', B-B' and C-C' in Fig. 5). In chrono-stratigraphic order, Table 2 provides a description of the lithology, age, grade and type of relative permeability, literature hydraulic conductivity, role, extension of each hydrogeological complex and, in simple form, the type of groundwater. Among the outcropping complexes, limestone-dolomite complex (ID 12) of the Mesozoic-Cenozoic Apennine platform domain is the most representative, covering 33.3 % of the area. It is followed by the pyroclastic deposits (ID 6), limestone (ID 10), detrital (ID 4) and pyroclastic-alluvial complex with extensions of 27.6 %, 19.5 %, 9.0 % and 4.6 %, respectively. The hydrogeological complexes with the smallest extensions include eluvial-colluvial (ID 1), lacustrine and marshy (ID 2), sandstone (ID 8), dolomite (ID 13) and marly limestone (ID 14) complexes, with coverages 2.7 %, 1.3 %, 0.9 %, 0.3 % and 0.3 %, respectively. In relation to the total surface (approximately 370 km<sup>2</sup>), the hydrogeological complexes characterized by high (52.8 %), medium (45.5 %) and low (1.3 %) degrees of relative permeability occupy areas of about 195, 168, and 4.80 km<sup>2</sup>, respectively. Among the outcropping hydrogeological complexes, the aquifers (94.4 %), aquitards (1.5 %), and aquicludes (1.2 %) occupy areas of about 349.3, 5.5, and 4.4 km<sup>2</sup>, respectively.

The Mesozoic-Cenozoic carbonate domain constitutes the basal aquifer, the turbiditic pre- and syn-orogenic deposits and Quaternary pyroclastic-alluvial deposits represent the lateral aquiclude and aquitard, respectively. The three hydrostratigraphic sections (see A-A', B-B' and C-C' in Fig. 5) show a thickness of about 2800 m and the deep geometry of the carbonate succession, tectonically juxtaposed with lower permeability units belonging to the domains of Lagonegro-Molise Basin and turbiditic pre- and syn-orogenic deposits.

Locally, some direct and inverse fault systems in north-eastern sector act as semipermeable barriers to groundwater flow directed towards the springs, establishing a typically basins-in-series system.

The piezometric contour lines of the groundwater model (Fig. 5) show an unconfined basal flow oriented towards the north-western, southern, and south-eastern edges. The water table is very deep, reaching up to about 1300 m b.g.l., with values variable approximately between about 350 and just below 30 m a.s.l. Hydraulic gradients range from  $6.32 \times 10^{-4}$  to  $1.03 \times 10^{-1}$  with an average value of  $2.01 \times 10^{-2}$ ; the highest values correspond to a groundwater drainage zone located in the central sector of the massif.

Due to the occurrence of groundwater divides, which partially coincide with a synclinal and anticlinal fold system (Fig. 5), five groundwater basins are delineated with distinct natural groundwater outlets. In addition to the groundwater basins of the Cancellò, S. Maria La Foce, Mercato, Palazzo, S. Marina di Lavarate and S. Mauro springs, two new groundwater basins were recognized. Their subsurface outflow is directed towards the pyroclastic-alluvial deposits of the Campanian plain through the locally highly transmissive piedmont karst aquifer of the Baiano valley (Fig. 5). Moreover, in the southern sector an interaction between the groundwater of the Solofrana plain and karst aquifer is certainly possible, in agreement with previous studies (Celico, 1983; Celico et al., 1980).

Currently, the active basal springs are S. Maria La Foce, Palazzo, Cerola, S. Marina di Lavarate, Laura and Labso springs, while those continuously monitored since 2021 by GORI SpA are only S. Maria La Foce and S. Marina di Lavarate, whose average discharge is equal to 1.70 m<sup>3</sup>/s and 1.80 m<sup>3</sup>/s, respectively.

In contrast, Mefito, Calabritto, Mercato and S. Mauro springs have been completely dry since the 1980s and 1990s, although Calabritto spring has been partially and temporarily reactivated in 2013 with a flow rate up to about 0.01 m<sup>3</sup>/s. In accordance with Meinzer's classification (Meinzer, 1923; 1927) these basal springs are classified as "cold gravity springs" of second and third magnitude, being the average discharge rate variables from 0.1 to 10 m<sup>3</sup>/s. Within the spring groundwater basins, a sub horizontal and laminar flow is present, that near springs is slightly ascending and oriented towards the Quaternary alluvial-pyroclastic deposits (see sections in Fig. 5). Due to their deep reservoir geometry, these spring basins contain significant volumes of groundwater reserves, in addition to the dynamic groundwater resources annually discharged by the springs.

In addition to basal springs, 137 high-altitude springs were censused, mainly located in the central and northern sectors (Fig. 5) at altitudes ranging from 160 and 1300 m a.s.l. and characterized by maximum discharges up to 0.040 m<sup>3</sup>/s and seasonal and perennial regimes. Based on Springer and Stevens (2009) classification, these are hanging and multi-habitat springs emerging from perched and unconfined aquifers in the limestone and limestone-dolomite complexes, and subordinately in detrital and pyroclastic deposits. Fed by a gravity-driven laminar flow, these springs are characterized by restricted dynamic groundwater resources, while the static deep reserves are not available. The genesis of these perched springs is controlled by stratigraphic and structural contacts within carbonate bedrock (e.g., the layer of Orbitolina marly limestone, and faults), as well as vertical variations of hydraulic conductivity within of the "pyroclastic soil-epikarst-carbonate bedrock" system (De Vita et al., 2003; Celico et al., 2010). This surficial heterogeneous system, acting as a temporary water storage tank, regulates the infiltration and evapotranspiration processes in the soil-plant-atmosphere system.

Well-developed karst landforms, such as endorheic areas, sinkholes, caves, and swallow holes, are mainly located in the southern sector. These karst forms exert significant control over groundwater recharge and transport of pollutants towards the springs; additionally, they influence ground instabilities, locally representing a new geohazard (e.g., flooding, soil collapse phenomena) in a karst environment already known for a high risk of landslide, sinkhole, and subsidence (Santo et al., 2008, 2019; Valente et al., 2021).

### 5.2. Updated water balance

At the aquifer scale, the study area is characterized by a homogeneous planimetric distribution of thermo-pluviometric stations (Fig. 6a). Conversely, an uneven altitude distribution was observed, as there is a lack of stations at altitudes higher than 800 m a.s.l. (Fig. 6b). The comparison between the hypsometric curve and the distribution of monitoring stations altitude shows that about 30 % of the recharge area with altitudes ranging from 800 and 1600 m a.s.l., lacks rain gauges and air temperature stations. Notwithstanding this structural gap in the regional basic climate network, also observed in other carbonate areas of the southern Apennine (Allocca et al., 2014), two linear regression models were implemented for precipitation and air temperature with altitude (Figs. 6c and 6d), by the following equations with high statistical significance:

$$P \text{ (mm)} = 1286 \times h \text{ (m a.s.l.)} + 960.96 \text{ (R}^2 = 0,85; \text{ Prob. F-Fisher} < 0.1 \text{ \%)}, \text{ and}$$

$$T \text{ (}^\circ\text{C)} = -0.0059 \times h \text{ (m a.s.l.)} + 16.871 \text{ (R}^2 = 0.86 \text{ Prob. F-Fisher} < 0.1 \text{ \%)}.$$

The equations were applied to develop distributed models of the precipitation, air temperature (Fig. 7a and b), and AET by application of Turc (1954) formula (Fig. 7c).

The distributed models (Fig. 7a and b) show a variation of precipitation from a minimum value of 993 mm/y to a maximum of about 2970 mm/y, with a mean value about 1702 mm/y (Fig. 7a; Table 3), while air temperature ranges from 7,6 to 16,7 °C, with a mean annual value about 13,4 °C (Fig. 7b; Table 3).

In Fig. 7c and d are reported both distributed models of AET estimated by Turc (1954) and MODIS satellite data. AET calculated by Turc (1954) formula varies from a minimum of 507 mm/y to a maximum of about 730 mm/y, with a mean value about 660 mm/y (Fig. 7c; Table 3), whereas estimated with MODIS satellite data varies from a minimum of 380 mm/y to a maximum of about 1100 mm, with a mean value about 725 mm/y (Fig. 7d; Table 3); in both cases, an AET value equal to 0 mm was assigned to urban areas or with absent vegetation. The variation ranges of AET with altitude and the differences in mean annual values depend on the approaches employed and spatial variability of air temperature, precipitation, and land use.

The GR values vary from 0 mm to 2449 mm (with a mean value of about 622 mm), and from 0 mm to 2265 mm (with a mean value about 588 mm) with Turc (1954) formula and MODIS satellite data, respectively. The highest GR values are at the highest altitudes, endorheic areas or with lower soil thickness or absent, whereas the lowest values generally are in the piedmont or urbanized areas. Overall, for the entire karst aquifer was estimated a GR variable from about 7,30 m<sup>3</sup>/s to 6,90 m<sup>3</sup>/s, respectively by AET Turc (1954)

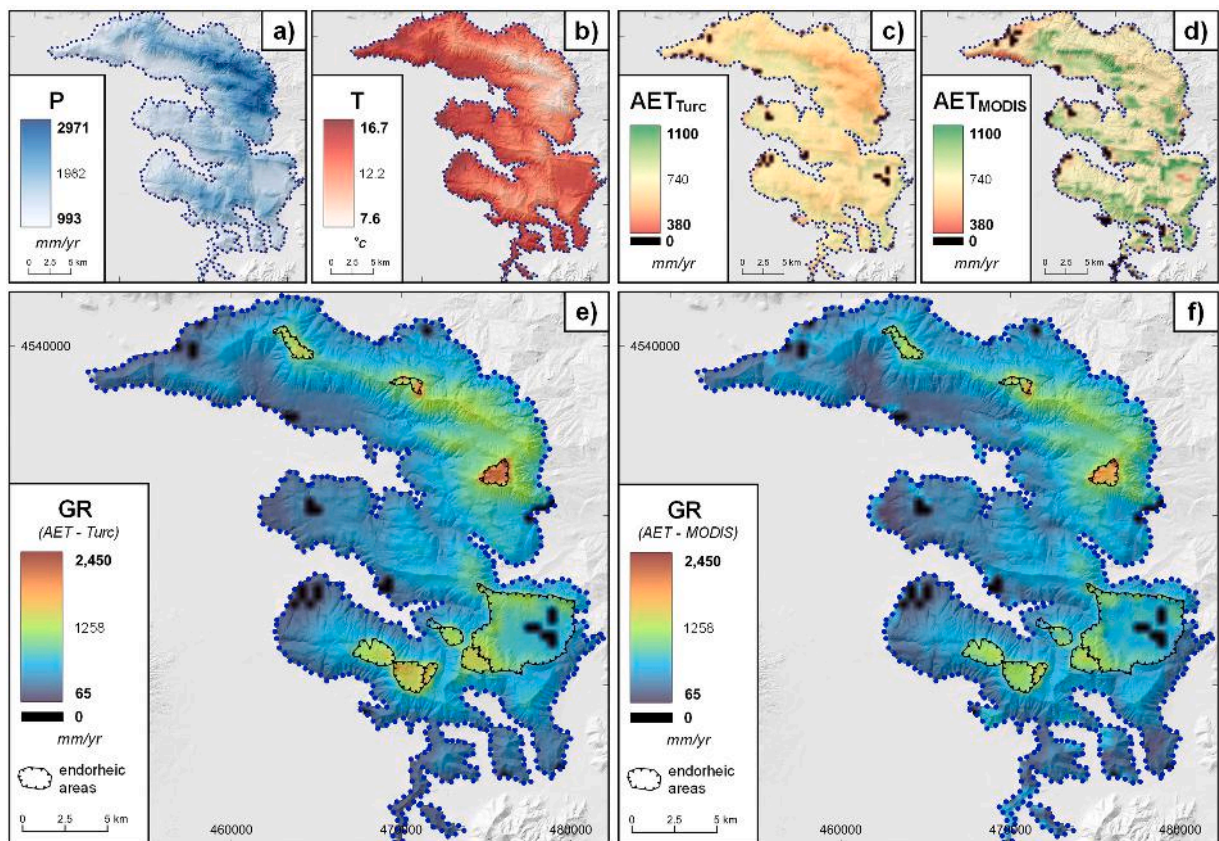


Fig. 7. Distributed models of: a) mean annual precipitation; b) mean annual air temperature; c) mean annual AET (Turc, 1954); d) mean annual AET (MODIS); e) mean annual GR (calculated by AET Turc); f) mean annual GR (calculated by AET MODIS).

**Table 3**

Updated water balances of Avella Mts. P, mean annual precipitation; T, mean annual air temperature; AET, mean annual actual evapotranspiration; GRC, groundwater recharge coefficient; GR, groundwater recharge; SGR, mean annual Specific Groundwater Recharge; (\*) average value.

Water balance	Method for AET	Area (km <sup>2</sup> )	Scale of analysis	Period	No. of meteorological stations		P (mm)	T (°C)	AET (mm)	GRC	GR (mm)	GR (m <sup>3</sup> /s)	SGR (m <sup>3</sup> /s/km <sup>2</sup> )		
					P	T									
1	Turc (1954)	370	~ 500 m resolution	2000÷2019	23	11	1702	13.4	660	0, 0.57 and 1	622	7.30	0.020		
2	MODIS data	370	~ 500 m resolution	2000÷2019	23	11	1702	13.4	725	(693*)	0, 0.57 and 1	588	6.90	(7.10*)	(0.020*)

formula and MODIS data, corresponding to mean annual SGR equal to about  $0.020 \text{ m}^3/\text{s}/\text{km}^2$  for the period 2000–2019 (Table 3). The results of water balance obtained by both approaches are mutually comparable, thus confirming the validity of dataset and approaches used. The very slightly difference among the values is probably linked to the different structure of the satellite data, which in urban areas estimates locally a higher actual evapotranspiration rate (Fig. 7a and b) for the small public and private green areas.

The new estimate of GR is certainly reliable because carried out by a more detailed hydrogeological conceptual model and a data-based ground and satellite integrated approach, considering the land use, soil type and other geomorphological factors that control groundwater recharge.

### 6. Discussion

The comparison between the preceding literature and new hydrogeological schemes (Fig. 8a, b and c) shows substantial differences and changes. The differences are linked not only to the more detailed analysis scale, but also to a new geological and hydrogeological dataset that allowed to define groundwater flow path and extension of groundwater basins of springs.

In disagreement with Civita et al. (1973), along the north-eastern edge the basal springs are absent, because the water table is very deep and barred by tectonic contact with turbiditic pre- and syn-orogenic deposits. The springs incorrectly interpreted as basal springs are fed by shallow lateral outflow within both Mesozoic-Cenozoic carbonate sequence and permeable detrital deposits overlying the turbiditic pre- and syn-orogenic units.

Unlike previous schemes, the carbonate hydrostructure is divided into five groundwater basins (Fig. 8c). This new aquifer compartmentalization highlights that Cancellò spring group, S. Maria La Foce and Palazzo springs have dimensionally smaller groundwater basins (Fig. 8c) as well as S. Marina di Lavorate and S. Mauro springs fed by an autonomous groundwater basin which includes the small limestone relief near the town of Roccapiemonte (Figs. 5 and 8c). Instead, it is quite clear that the total disappearance of some basal springs (e.g. Mefito, Calabricito, Mercato and S. Mauro springs) is due to mainly anthropogenic factors linked to excessive exploitation of the aquifer at the local scale (Figs. 1d, 2 and 8c), as probably also the decrease in the average flow rate of the S. Maria La Foce spring, from  $2.60 \text{ m}^3/\text{s}$  measured in the 1960s–1970s (Celico, 1983; Allocca et al., 2007) to  $1.70 \text{ m}^3/\text{s}$ , recorded currently.

The comparison between the previous and new water balance (Fig. 8d) highlights significant differences and changes linked in addition to the scale of analysis, method and dataset used, also reduction in the precipitation and recharge, as well as increase of air temperature and actual evapotranspiration.

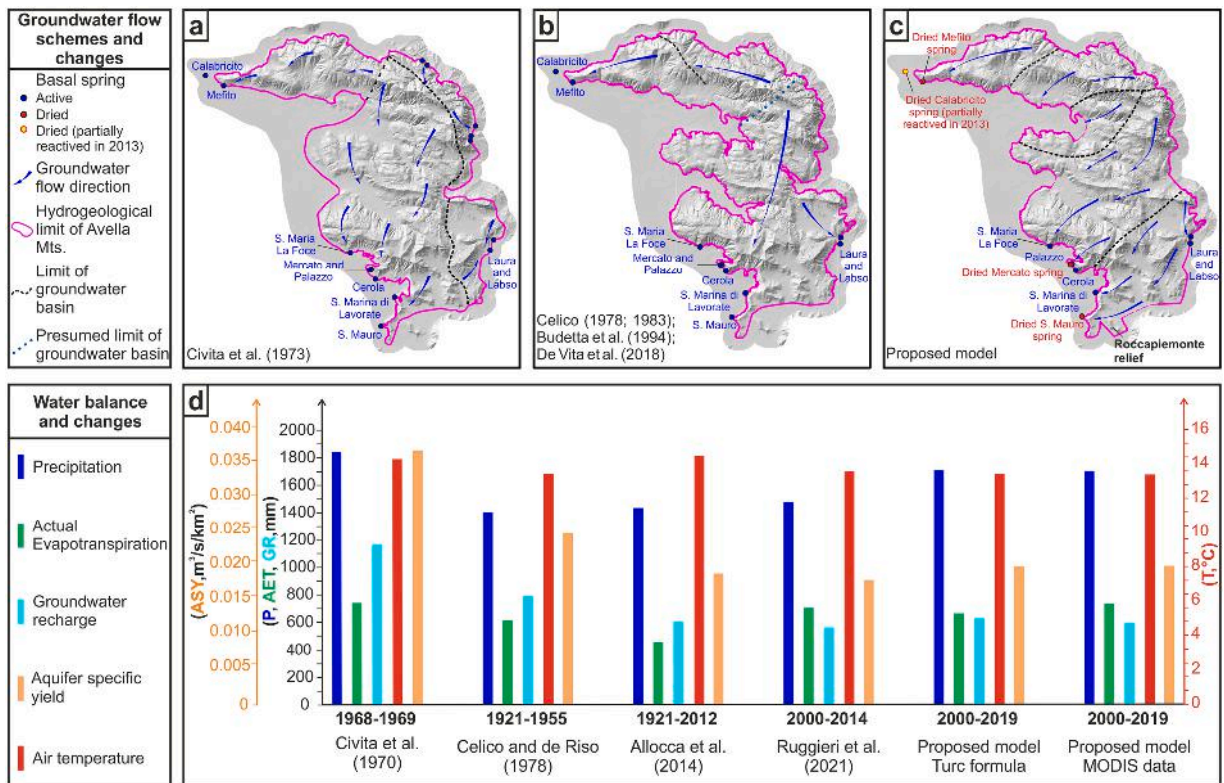


Fig. 8. Comparison between previous schemes a) Civita et al. (1973); b) Celico (1978); (1983); Budetta et al. (1994); De Vita et al. (2018); and c) proposed hydrogeological model; d) Comparison between previous and proposed water balances.

y) (Table 3; Figs. 7d and 8d), while the GR calculated by Civita et al. (1970) equal to 1200 mm/y (Table 1 e Fig. 8d) is probably overestimated, having used a maximum value of the GRC (equal to 1) and recorded a peak of annual precipitation in the 1968–1969 hydrological year (Fig. 8d). More contained are the differences with other previous estimates carried out by Celico and de Riso (1978), Allocca et al. (2014) and Ruggieri et al. (2021) equal to about 790, 602 and 559 mm/y, respectively (Table 1; Fig. 8d). However, on the long term a decreasing trend of the mean GR (from 1200, 790 mm to 605 mm/y) and mean annual SGR (from 0.037, 0.025–0.020 m<sup>3</sup>/s/km<sup>2</sup>) is observed (Fig. 8d). These trends are probably due to decadal and inter-annual variability of precipitation, teleconnected with the North Atlantic Oscillation (De Vita et al., 2012; Longobardi and Boulariah, 2022), and a change in rainfall regime, as well as increase in extreme rainfall events observed at the national and regional scale (e.g., Brunetti et al., 2004; Caporali et al., 2020; Capozzi et al., 2023; Avino et al., 2024) which certainly does not favor groundwater recharge processes.

The differences and changes found in the new conceptual model and water balance have important implications for current and future groundwater management, as well as waterwork systems security and groundwater-dependent ecosystems. In this new hydrogeological scenario under climate change (e.g., Bucchignani et al., 2016; Bonanno et al., 2018; Faggian, 2021) and increasing human pressure, a change in groundwater management is fundamental to prevent further environmental changes for the springs, groundwater-dependent ecosystems and groundwater quality (Gleeson et al., 2012).

The current management is lacking in coordination between public bodies and private subjects. Moreover, is a priority to implement by local authorities the water user register or inventory which is currently missing or incomplete. Some next steps of the study were planned to assess of the current exploitation status of the aquifer. Automatic multiparametric (e.g., piezometric level, spring discharge, water temperature) monitoring stations were installed into the main springs tapping works, wells and well fields used for drinking water. Withdrawals data for private uses, partially collected from local authorities, will be integrated with new field surveys. This will allow validate the water balance and reduce uncertainty of the multi-approach estimations (e.g., Guardiola-Albert et al., 2015; Zekri et al., 2015) as well as to quantify the water stress degree of karst aquifer. In addition, numerical models in steady and transient state (e.g., SWB and SWAT) are in phase of implementation for the simulation of future scenarios considering different natural and anthropogenic forcing (e.g., decrease of rainfall and recharge, increase of groundwater abstractions, environmental needs).

A comprehensive hydrogeological conceptual model and the integration of regional climate models and numerical simulation could support decision-makers in groundwater management (e.g., Nayak et al., 2015; Mamo et al., 2021; Singh et al., 2019; Brussolo et al., 2022), also to predict possible water crisis scenarios and establish a multiscale aquifer exploitation threshold.

## 7. Conclusions

Based on a systematic literature review and new geological and piezometric data, in this study we propose a novel hydrogeological conceptual model of Avella Mts. at the 1:50,000 scale, and a double estimate of groundwater recharge carried out by ground-based hydrological and remote sensing data referred to the period 2000–2019.

The main results related to the new hydrogeological conceptual model and the updated water balance are summarized as follows:

- 15 hydrogeological complexes belonging to 4 hydrogeological domains have been identified.
- Limestone-dolomite complex (ID 12) of the Mesozoic-Cenozoic Apennine platform domain is the most representative (33.3 % of the karst area).
- Hydrogeological complexes (ID 10, 12 and 13) of the Mesozoic-Cenozoic carbonate domain constitute the basal aquifer, while the turbiditic pre- and syn-orogenic deposits and Quaternary pyroclastic-alluvial deposits represent the lateral aquiclude and aquitard, respectively.
- The local pattern of tectonic discontinuities determines a typically basins-in-series system for the deep structure of the aquifer, also influencing the basal groundwater flow, which is mostly oriented towards the north-western, southern, and south-eastern edges of the massif.
- 5 groundwater basins are recognized and 3 of them feed basal springs tapped for drinking water by different aqueduct systems; these basal springs are experiencing a decrease in discharge rate compared to historical data due to natural and anthropogenic factors.
- In addition to basal springs, 137 high-altitude springs are mainly located in the central and northern sectors of the massif, fed by local perched (epikarst, detrital and pyroclastic) aquifers.
- The estimated groundwater recharge of the whole aquifer varies from about 7,30 m<sup>3</sup>/s to 6,90 m<sup>3</sup>/s, corresponding to a mean annual SGR equal to 0.020 m<sup>3</sup>/s/km<sup>2</sup>; the highest values of infiltration occur at the highest altitudes, in endorheic areas, or where soil thickness is lower or absent.

The new hydrogeological conceptual model, along with the updated estimation of groundwater recharge, provides a fundamental basis for: (i) supporting regional and local water authorities in the sustainable management of this strategic aquifer, which is crucial for the health, economy, and environment of a large area of the Campania region, and (ii) evaluating the effects of climate change on groundwater recharge and the increasing human pressure on groundwater resource.

## CRedit authorship contribution statement

**Pantaleone De Vita:** Writing – review & editing, Writing – original draft, Validation, Supervision, Resources, Methodology,



Investigation, Formal analysis, Data curation. **Paola Petrone**: Writing – original draft, Validation, Software, Methodology, Formal analysis, Data curation. **Pasquale Allocca**: Validation, Software, Methodology, Formal analysis, Data curation. **Marsiglia Palmira**: Validation, Software, Methodology, Formal analysis, Data curation. **Delia Cusano**: Validation, Software, Methodology, Formal analysis, Data curation. **Silvio Coda**: Writing – original draft, Validation, Software, Methodology, Formal analysis, Data curation. **Vincenzo Allocca**: Writing – review & editing, Writing – original draft, Validation, Supervision, Resources, Project administration, Methodology, Investigation, Formal analysis, Data curation, Conceptualization. **Daniele Lepore**: Software, Methodology, Data curation.

## Declaration of Competing Interest

The authors declare that they have no known competing financial interests or personal relationships that could have appeared to influence the work reported in this paper.

## Data availability

Data will be made available on request.

## Acknowledgements

The research was undertaken and funded within Research Agreement entitled “*Convenzione di Studio, Ricerca e Supporto tecnico-scientifico relativa alle Sorgenti e opera di captazione di S. Maria la Foce, Mercato-Palazzo, S. Marina di Lavorate e San Mauro (Sarno e Nocera Inferiore – SA) e di Suppezzo (Castellammare di Stabia – NA)*” (Scientific Coordinator: V. Allocca; D. Calcaterra; P. De Vita) signed in July, 2019 (Prot. 2019/0081394 del 30/07/2019, Dipartimento di Scienze della Terra, dell’Ambiente e delle Risorse) between the Department of Earth Sciences, Environment and Resources, University of Naples Federico II and the GORI SpA. This research was also funded by European Union - NextGenerationEU - Mission 4 “Education and Research” - Component 2 “From Research to Business” - Investment 3.1 “Fund for the realization of an integrated system of research and innovation infrastructures” - Project IR0000037 - GeoSciences IR., and supported by the Earth Sciences, Environment and Resources, PhD Program of the University of Naples Federico II (XXXIV and XXXVII cycle). The authors thank the two Editors and three anonymous reviewers for their precious comments and suggestions.

## References

- Allocca, V., Celico, F., Celico, P., De Vita, P., Fabbrocino, S., Mattia, S., Monacelli, G., Musilli, I., Piscopo, V., Scalise, A.R., Summa, G., and Tranfaglia, G., 2007. Illustrative Notes of the Hydrogeological Map of Southern Italy. Istituto Poligrafico e Zecca dello Stato, Rome, 1–211, ISBN 88-448-0223-6.
- Allocca, V., Aquino, S., Esposito, L., Celico, P., 2008. The groundwater of the Irpinia area (Southern Italy). *Current Knowledge and Future Perspectives. L'ACQUA* 6 (2008), 39–66.
- Allocca, V., Manna, F., De Vita, P., 2014. Estimating annual groundwater recharge coefficient for karst aquifers of the southern Apennines (Italy). *Hydrol. Earth Syst. Sci.* 18 (2), 803–817.
- Allocca, V., De Vita, P., Manna, F., Nimmo, J.R., 2015. Groundwater recharge assessment at local and episodic scale in a soil mantled perched karst aquifer in southern Italy. *J. Hydrol.* 529, 843–853.
- Allocca, V., Marzano, E., Tramontano, M., Celico, F., 2018. Environmental impact of cattle grazing on a karst aquifer in the southern Apennines (Italy): Quantification through the grey water footprint. *Ecol. Indic.* 93 (2018), 830–837.
- Avino, A., Cimorelli, L., Furcolo, P., Noto, L.V., Pelosi, A., Pianese, D., Villani, P., Manfreda, S., 2024. Are rainfall extremes intensifying in Southern Italy? *J. Hydrol.* <https://doi.org/10.1016/j.jhydrol.2024.130684>.
- Beck, H.E., Zimmermann, N.E., McVicar, T.R., Vergopolan, N., Berg, A., Wood, E.F., 2018. Present and future Köppen-Geiger climate classification maps at 1-km resolution (Article). *Sci. Data* 5, 180214. <https://doi.org/10.1038/sdata.2018.214>.
- Ben Saad, E., Ben Alaya, M., Taupin, J.D., Patris, N., Chaabane, N., Souissi, R., 2018. A Hydrogeological Conceptual Model Refines the Behavior of a Mediterranean Coastal Aquifer System: A Key to Sustainable Groundwater Management (Grombalia, NE Tunisia) (<https://doi.org/>). *Hydrology* 2023 10, 180. <https://doi.org/10.3390/hydrology10090180>.
- Bonanno, R., Faggian, P., 2018. Changes in the precipitation regime over the Italian Peninsula and their possible impacts on the electric system. *Tethys J. Mediterr. Meteorol. Climatol.* 2018 15, 18–30.
- Brunetti, M., Maugeri, M., Monti, F., Nanni, T., 2004. Changes in daily precipitation frequency and distribution in Italy over the last 120 years. *J. Geophys. Res.* 2004 109, D05102.
- Brussolo, E., Palazzi, E., von Hardenberg, J., Masetti, G., Vivaldo, G., Previati, M., Canone, D., Gisolo, D., Bevilacqua, I., Provenzale, A., Ferraris, S., 2022. Aquifer recharge in the Piedmont Alpine zone: Historical trends and future scenarios. *Hydrol. Earth Syst. Sci.* 26 (2), 407–427. <https://doi.org/10.5194/hess-26-407-2022>.
- Bucchignani, E., Montesarchio, M., Zollo, A.L., Mercogliano, P., 2016. High-resolution climate simulations with COSMO-CLM over Italy: Performance evaluation and climate projections for the 21st century. *Int. J. Climatol.* 2016 36, 735–756.
- Budetta, P., Celico, P., Corniello, A., de Riso, R., Ducci, D., Nicotera, P., 1994. Carta idrogeologica della Campania 1: 200.000 – Memoria illustrativa. *Atti Convegno Int. Geoingegneria: “Difesa e Valorizzazione dei suoli e degli Acquiferi”*, 1994, 565–586, Torino.
- Busetto, L., Ranghetti, L., 2016. MODISr: An R package for automatic preprocessing of MODIS Land Products time series. *Comput. Geosci.* 97, 40–48. <https://doi.org/10.1016/j.cageo.2016.08.020>.
- Caporali, E., Lompi, M., Pacetti, T., Chiarello, V., Faticchi, S., 2020. A review of studies on observed precipitation trends in Italy. *Int. J. Climatol.* 2021 41 (Suppl. 1), E1–E25. <https://doi.org/10.1002/joc.6741>.
- Capozzi, V., Rocco, A., Annella, C., Cretella, V., Fusco, G., Budillon, G., 2023. Signals of change in the Campania region rainfall regime: An analysis of extreme precipitation indices (2002–2021). *e2168 Meteorol. Appl.* 30, 2023. <https://doi.org/10.1002/met.2168>.
- Celico, F., Naclerio, G., Bucci, A., Nerone, V., Capuano, P., Carcione, M., Allocca, V., Celico, P., 2010. Influence of pyroclastic soil on epikarst formation: a test study in southern Italy. *Terra Nova* 22, 110–115.
- Celico, P., 1978. Schema idrogeologico dell’Appennino carbonatico centromeridionale. *Mem. e Note Ist. di Geol. Appl.* 14, 1–97 (Napoli).

- Celico, P., 1983. Idrogeologia dei massicci carbonatici, delle piane quaternarie e delle aree vulcaniche dell'Italia centro-meridionale (Marche e Lazio meridionale, Abruzzo, Molise e Campania). Quaderni della Cassa per il Mezzogiorno 4 (2), 1–203, Roma.
- Celico, P., 1986. Prospezioni Idrogeologiche. Liguori Editore, Napoli, Italia, pp. 1–735. Vol. I, ISBN 88-207-1331-4.
- Celico, P., de Riso, R., 1978. Il ruolo della Valle Caudina nella idrogeologia del Casertano e del Sarnese (Campania). Mem. e Note Ist. Geol. Appl. 14, 1–24.
- Celico, P., De Gennaro, M., Ferreri, M., Ghiara, M., Russo, D., Stanzione, D., Zenone, F., 1980. Il margine orientale della Piana Campana: indagini idrogeologiche e geochimiche. Period. Miner 49, 241–270.
- Chen, Z., Auler, A.S., Bakalowicz, M., Drew, D., Griger, F., Hartmann, J., Jiang, G., Moosdorf, N., Richts, A., Stevanovic, Z., Veni, G., Goldscheider, N., 2017. The world karst aquifer mapping project: concept, mapping procedure and map of Europe. Hydrogeol. J. 25 (3), 771–785.
- Civita, M., 2005. Idrogeologia applicata e ambientale. Casa Editrice Ambrosiana, pp. 1–800. ISBN: 8808087417.
- Civita M., de Riso R., Nicotera P., 1970. Sulla struttura idrogeologica alimentante dei sorgenti del F. Sarno e le falde pedemontane profonde della parte sud-orientale della Conca Campana. Atti I Convegno Internazionale sulle Acque Sotterranee, IAH, 1–24. Palermo, 6-8 Dicembre 1970.
- Civita M., de Medici G.B., de Riso R., Nicotera P., Nota d'Elogio E., 1973. Memoria descrittiva della carta idrogeologica della Campania nord-occidentale. Atti II Convegno Internazionale sulle Acque Sotterranee, IAH, 1–39. Palermo, 28 Aprile-2 Maggio 1970.
- Coutagne, A., 1954. Quelques considérations sur le pouvoir évaporant de l'atmosphère, le déficit d'écoulement effectif et le déficit d'écoulement maximum. La Houille Blanc 1954, 360–374.
- Cusano, D., Coda, S., De Vita, P., Fabbrocino, S., Fusco, F., Lepore, D., Nicodemo, F., Pizzolante, A., Tufano, R., Allocca, V., 2023. Comparison of methods for assessing groundwater vulnerability in karst aquifers: the case study of Termino Mt. aquifer (Southern Italy). Sustain. Environ. Res. (2023) 33, 42. <https://doi.org/10.1186/s42834-023-00204-8>.
- Cusano, D., Lepore, D., Allocca, V., De Vita, P., 2024. Control of soil mantle thickness and land cover types on groundwater recharge of karst aquifers in Mediterranean areas. J. Hydrol. 630 (2024), 130770.
- De Vita, P., Agrello, D., Ambrosino, F., De Luzio, E., 2003. Caratterizzazione del sistema idrogeologico superficiale coltre piroclastica-substrato carbonatico nella dorsale dei Monti di Sarno (Campania). Quad. di Geol. Appl. 2 (2003), 49–69.
- De Vita, P., Allocca, V., Manna, F., Fabbrocino, S., 2012. Coupled decadal variability of the North Atlantic Oscillation, regional rainfall and karst spring discharges in the Campania region (southern Italy). Hydrol. Earth Syst. Sci. 16 (5), 1389–1399.
- De Vita, P., Allocca, V., Celico, F., Fabbrocino, S., Mattia, C., Monacelli, G., Musilli, I., Piscopo, V., Scalise, A.R., Summa, G., Tranfaglia, G., Celico, P., 2018. Hydrogeology of continental southern Italy. J. Maps 14 (2), 230–241.
- Faggian, P., 2021. Future Precipitation Scenarios over Italy. Water 2021 13, 1335. <https://doi.org/10.3390/w13101335>.
- Ford, D., Williams, P., 2007. Karst Hydrogeology and Geomorphology. John Wiley & Sons Ltd, Chichester, UK, p. 576. <https://doi.org/10.1002/9781118684986>. Vol. 1.
- Freeze, R.A., Cherry, J.A., 1979. Groundwater. Prentice-Hall, Inc, Englewood Cliffs, New Jersey 07632. ISBN 0-13-365312-9.
- Fusco, F., Allocca, V., De Vita, P., 2017. Hydro-geomorphological modelling of ash-fall pyroclastic soils for debris flow initiation and groundwater recharge in Campania (southern Italy). Catena 2017 158, 235–249.
- Gleeson, T., Wada, Y., Bierkens, M.F.P., van Beek, L.P.H., 2012. Water balance of global aquifers revealed by groundwater footprint. Article 7410. Nature 488 (7410) <https://doi.org/10.1038/nature11295>.
- Goldscheider, N., 2019. A holistic approach to groundwater protection and ecosystem services in karst terrains. Carbonates Evaporites 34 (4), 1241–1249.
- Goldscheider, N., Chen, Z., Auler, A.S., Bakalowicz, M., Broda, S., Drew, D., Hartmann, J., Jiang, G., Moosdorf, N., Stevanovic, Z., Veni, G., 2020. Global distribution of carbonate rocks and karst water resources. Hydrogeol. J. (2020) 28, 1661–1677.
- Guardiola-Albert, C., Martos-Rosillo, S., Pardo-Igúzquiza, E., Durán Valsero, J.J., Pedrera, A., Jiménez-Gavilán, P., Liñán Baena, C., 2015. Comparison of Recharge Estimation Methods During a Wet Period in a Karst Aquifer. Groundwater 53 (6), 885–895. <https://doi.org/10.1111/gwat.12310>.
- ISPRA, 2017. Geological maps of Italy, scale 1:50,000. Sheets 431, 432, 448, 449, 466, 467, 485. ISPRA – Istituto Superiore per la Protezione e la Ricerca Ambientale, Servizio Geologico d'Italia. Retrieved from <http://www.isprambiente.gov.it/Media/carg/campania.html>.
- Lancia, M., Petitta, M., Zheng, C., Saroli, M., 2020. Hydrogeological insights and modelling for sustainable use of a stressed carbonate aquifer in the Mediterranean area: From passive withdrawals to active management. J. Hydrol.: Reg. Stud. 32 (2020), 100749.
- Longobardi, A., Boulariah, O., 2022. Long-term regional changes in inter-annual precipitation variability in the Campania Region, Southern Italy. Theor. Appl. Climatol. (2022) 148, 869–879.
- Mamo, S., Birhanu, B., Ayenew, T., Taye, G., 2021. Three-dimensional groundwater flow modeling to assess the impacts of the increase in abstraction and recharge reduction on the groundwater, groundwater availability and groundwater-surface waters interaction: A case of the rib catchment in the Lake Tana sub-basin of the Upper Blue Nile River, Ethiopia. J. Hydrol.: Reg. Stud. 35, 100831 <https://doi.org/10.1016/j.ejrh.2021.100831>.
- Maxey, G.B., 1964. Hydrostratigraphic units. J. Hydrol. 2, 124–129.
- Meinzer, O.E., 1923. Outline of ground-water hydrology, with definitions. U.S. Geological Survey Water-Supply Paper 494, 1-71, Washington DC.
- Meinzer, O.E., 1927. Large springs in the United States. U.S. Geological Survey Paper 557, 1-94, Washington DC.
- Monteith, J.L., 1965. Evaporation and environment. Symp. Soc. Exp. Biol. 19, 205–234.
- Mu, Q., Zhao, M., Running, S.W., 2011. Improvements to a MODIS global terrestrial evapotranspiration algorithm. Remote Sens. Environ. 115 (8), 1781–1800.
- Nayak, P.C., Wardlaw, R., Kharya, A.K., 2015. Water balance approach to study the effect of climate change on groundwater storage for Sirhind command area in India. Int. J. River Basin Manag. 13 (2), 243–261. <https://doi.org/10.1080/15715124.2015.1012206>.
- Nicotera, P., Civita, M., 1969b. Indagini idrogeologiche per la captazione delle sorgenti S. Marina di Lavorate (Sarno). Mem. e Note Ist. Geol. Appl. (1969) Vol. 11, 1–50 (Napoli).
- Nicotera, P., Civita, M., 1969a. Ricerche idrogeologiche per la realizzazione delle opere di presa delle sorgenti Mercato e Palazzo in Sarno (Campania). Mem. e Note Ist. Geol. Appl. (1969) Vol. 11, 1–59 (Napoli).
- Ruggieri, G., Allocca, V., Borfecchia, F., Cusano, D., Marsiglia, P., De Vita, P., 2021. Testing Evapotranspiration Estimates Based on MODIS Satellite Data in the Assessment of the Groundwater Recharge of Karst Aquifers in Southern Italy. Water 13 (2), 118, 2021.
- Running, S., Mu, Q., Zhao, M., Moreno, A., 2021. MODIS/Terra Net Evapotranspiration Gap-Filled Yearly L4 Global 500m SIN Grid V061 [Data set]. Accessed 2023-12-01 from NASA EOSDIS Land Process. Distrib. Act. Arch. Cent. <https://doi.org/10.5067/MODIS/MOD16A3GF.061>.
- Santo, A., Prete, S., Giulivo, I., 2008. Nuove ipotesi sulla formazione dei piping sinkhole in aree alluvionali: il caso della piana di Forino (Avellino, Campania). Ital. J. Quat. Sci. 21 (2), 395–408, 2008.
- Santo, A., Santangelo, N., De Falco, M., Forte, G., Valente, E., 2019. Cover collapse sinkhole over a deep buried carbonate bedrock: The case study of Fossa San Vito (Sarno - Southern Italy). Geomorphology 345 (2019), 106838. <https://doi.org/10.1016/j.geomorph.2019.106838>.
- Seaber, P.R., 1988. Hydrostratigraphic units. In: Back, W., Rosenschein, J.R., Seaber, P.R. (Eds.), Hydrogeology: The Geology of North America, Volume O-2. Geological Society of America. <https://doi.org/10.1130/DNAG-GNA-02>.
- Singh, A., Panda, S.N., Uzokwe, V.N.E., Krause, P., 2019. An assessment of groundwater recharge estimation techniques for sustainable resource management. Groundw. Sustain. Dev. 9, 100218 <https://doi.org/10.1016/j.gsd.2019.100218>.
- Springer, A.E., Stevens, L.E., 2009. Spheres of discharge of springs. Hydrogeol. J. (2009) 17, 83–93. <https://doi.org/10.1007/s10040-008-0341-y>.
- Sun, W., Song, J., Yang, W., Zheng, Y., Li, C., Kuang, D., 2020. Distribution of carbonate rocks and variation analysis of karst water resources in China. Carbonates Evaporites (2020) 35, 121. <https://doi.org/10.1007/s13146-020-00657-7>.
- Thornthwaite, C.W., Mather, J.R., 1955. The Water Balance. Publ. Climatol., 1955 8, 1–104.
- Tufano, R., Allocca, V., Coda, S., Cusano, D., Fusco, F., Nicodemo, F., Pizzolante, A., De Vita, P., 2020. Groundwater vulnerability of principal aquifers of the Campania region (southern Italy). J. Maps, 2020 16 (2), 565–576.
- Turc, L., 1954. Le bilan d'eau des sols: Relations entre les précipitations, l'évaporation et l'écoulement. Ann. Agron. 1954 5, 491–595.

- Valente, E., Allocca, V., Riccardi, U., Camanni, G., Di Martire, D., 2021. Studying a Subsiding Urbanized Area from a Multidisciplinary Perspective: The Inner Sector of the Sarno Plain (Southern Apennines, Italy). *Remote Sens.* 2021 13, 3323. <https://doi.org/10.3390/rs13163323>.
- Vitale, S., Ciarcia, S., 2018. Tectono-stratigraphic setting of the Campania region (southern Italy). *J. Maps*, 2018 14 (2), 9–21.
- Zekri, S., Triki, C., Al-Maktoumi, A., Bazargan-Lari, M.R., 2015. An Optimization-Simulation Approach for Groundwater Abstraction under Recharge Uncertainty. *Water Resour. Manag.* 29 (10), 3681–3695. <https://doi.org/10.1007/s11269-015-1023-x>.